SAE International

Cylinder Cooling for Improved Durability on an Opposed-Piston Engine

2012-01-1215
Published
04/16/2012

Patrick Lee
Achates Power Inc.

Michael Wahl
Achates Power Inc

doi:10.4271/2012-01-1215

ABSTRACT

The cooling system design for a two-stroke, opposed-piston (OP) engine is substantially different from that of a conventional four-stroke engine as the opposed-piston engine requires efficient cooling at the center of the cylinder where the heat load is highly concentrated. A thermally efficient design ensures engine durability by preserving the oil film at the top ring reversal zone. This is achieved by limiting the surface temperature of the liner to below 270° C at this location. Various water jacket designs have been analyzed with computational fluid dynamics (CFD) using a "discretized" Nusselt number approach for the gas side heat flux prediction. With this method, heat transfer coefficients are computed locally given the flow field of the combustion gases near the liner surface and then multiplied by the local gas/liner temperature difference to generate the heat flux distribution into the cylinder liner. The heat flux is then averaged over the cycle before being applied as a boundary condition to the CFD simulation. The baseline design consists of a simple water jacket with coolant flowing axially from the inlet near the intake port to the outlet near the exhaust port. This approach yields uneven cooling both longitudinally and circumferentially about the cylinder liner. A greatly improved thermal response has been achieved by introducing the coolant at the hot center section of the liner with roughly half of the coolant flowing toward either end of the cylinder. A detailed analysis shows that liner surface temperatures well below 270° C can be achieved for an engine with a power density of 50kW/liter by carefully optimizing the coolant velocities in the center section of the liner.

INTRODUCTION

Opposed-piston, two-stroke engines were conceived in the late 1800s in Europe and subsequently developed in multiple countries for a wide variety of applications [1, 2, 3, 4, 5]. An excellent summary of the history of opposed-piston engines can be found in [1]. Produced initially for their manufacturability, high power density and fuel efficiency, opposed-piston, two-stroke engines demonstrated their versatility in a variety of applications including aircraft, ships, tanks, trucks and locomotives and maintained their presence throughout most of the twentieth century. Historically, all types of engines have faced a number of technical challenges related to emissions, fuel efficiency, cost and durability-to name a few-and these challenges have been more easily met by four-stroke engines, as demonstrated by their widespread use. However, the economic pressure due to continuously rising fuel costs has led to a re-examination of the fundamental limits of fuel efficiency in internal combustion engines. Opposed-piston, two-stroke engines, with their inherent thermodynamic advantage, have emerged as a promising alternative.

Opposed-piston (OP), two-stroke engines have a number of fundamental design advantages over common four-stroke engines as discussed in [6]. In particular, the two-stroke cycle's double firing frequency gives designers the choice of either increasing power density or decreasing peak cylinder pressure for a given torque requirement. Lower cylinder pressures lead to lower mechanical stress on engine components, which can therefore be designed lighter, and it also reduces friction. Lower gas temperatures lead to decreased NO_X formation during combustion, which lowers

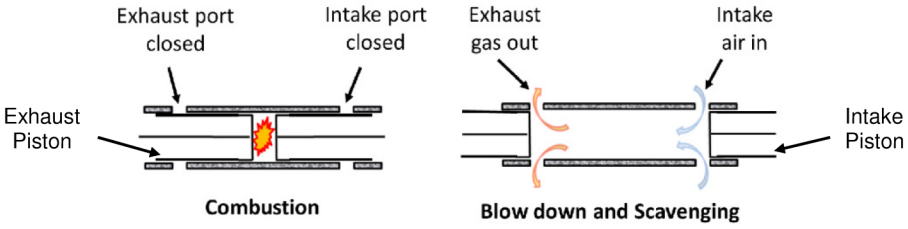

Figure 1. Opposed-Piston Engine Operation

the requirement for exhaust gas recirculation (EGR) or NO_X aftertreatment devices. Alternatively, increased power density leads directly to smaller engine size and weight, both of which are beneficial to vehicle fuel economy and manufacturing costs.

Relative to durability, the two-stroke cycle's double firing frequency poses a cooling challenge, since the cylinder liner is not as effectively cooled by the fresh charge as with a four-stroke engine. In order to keep the liner temperature at an acceptable level for the oil film to survive and in order to minimize bore distortions, excellent cylinder cooling is a prerequisite for durability. This paper describes the analysis methodology that was used to implement an efficient cylinder cooling scheme for an opposed-piston engine to ensure superior durability.

Opposed-piston engines are piston ported, i.e., the intake and exhaust ports are exposed as each piston moves past the ports as illustrated in Figure 1.

The gas exchange phase during scavenging induces a flow field inside the cylinder that persists long after the ports close and drives much of the heat transfer on the hot side. Since combustion occurs near the center of the cylinder while the two pistons are at or near TDC, the heat flux from combustion is concentrated at the center of the cylinder, as shown in Figure 2.

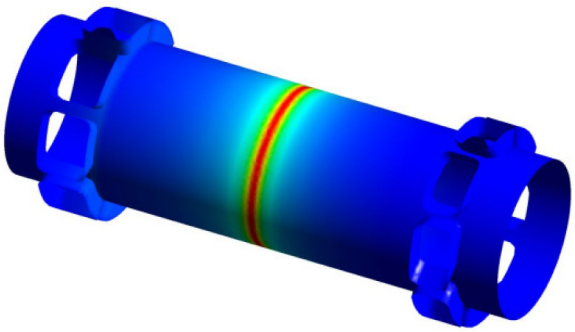

Figure 2. Heat Flux on the Hot Side Boundary of the Cylinder and Intake and Exhaust Ports

A substantial reduction of thermal distortion and thermally induced stress in the cylinder can increase engine power and durability. Effectively tailored cylinder cooling limits the maximum temperature at top ring reversal and also significantly reduces non-uniform bore distortion.

METHOD

To analyze the thermal response of the cylinder, a Conjugate Heat Transfer (CHT) analysis was performed using the computational fluid dynamics (CFD) code ANSYS CFX. Due to the nature of the in-cylinder charge motion, it was recognized that the convective heat transfer on the hot side dominates other effects such as radiation. Therefore, the hot side boundary conditions were determined using a heat flux model based on a Nusselt number correlation for the heat transfer coefficient providing a viable and convenient alternative to a 3-D combustion CFD analysis when evaluating various cylinder coolant designs.

Dent and Sulaiman [7] investigated the applicability of using a forced convective turbulent heat transfer correlation for flow over a flat plate to predict the convective heat flux in a high swirl direct injection diesel engine. In this investigation, the heat transfer correlation was based on the Nusselt number as derived by Kreith [8]. Their experiments showed two distinct zones in the piston-cylinder combustion space. A high temperature zone formed by the piston bowl and cylinder head, and a low temperature zone in the piston squish region. They found reasonable agreement with the correlation if measured cylinder air motion data was used and allowances were made for increased swirl during firing. Differences in the local gas temperature between the bowl and squish zones was also accounted for.

Other correlations for the heat transfer coefficient have been used in the past for direct injection diesel engines, such as Annand [9], Woschni [10], and Le Feuvre et al. [11]. The correlation used by Annand [9] is very similar to Dent and Sulaiman [7]. An important difference is Dent and Sulaiman [7] used the swirl velocity as the characteristic velocity and the bore circumference as the characteristic length in the Reynold's number. Annand [9] and Woschni [10] used the mean piston speed as the characteristic velocity and the bore diameter as the characteristic length. However, the predominant in-cylinder charge motion in a uniflow scavenged opposed-piston engine is better characterized by swirl velocity than mean piston speed. To keep the

characteristic length compatible with the characteristic velocity, it is appropriate to use the bore circumference as the characteristic length instead of the bore diameter. In light of the results given by Dent and Sulaiman [7] and the similarity of forced vortex flow to the in-cylinder charge motion that occurs in an opposed-piston cylinder, deriving the heat transfer coefficient from considering forced turbulent flow over a flat plate was considered reasonable for estimating heat flux into the cylinder wall.

HEAT FLUX MODEL

The hot side boundary conditions are based on a cycle averaged heat flux from the hot combustion gases into the cylinder wall. The heat entering the cylinder wall has traditionally been expressed as:

$$\dot{Q}_w = h\,A(T_g - T_w) \tag{1}$$

where $\dot{Q}_w$ is the heat flux into the cylinder wall, h is the convective heat transfer coefficient, and A is the surface area of the cylinder wall. T_W and T_g are the wall and mean gas temperatures, respectively.

Heat Release from Combustion

Combustion was modeled using an adiabatic single zone thermodynamic model, thus localized heating from the flame front and radiation, as well as heat loss to the piston crown, were not considered. The temperature rise caused by compression and heat release from combustion was treated as time varying but uniform throughout the combustion volume.

At intake port closing, the temperature of the gas in the cylinder was assumed to be the temperature of the incoming fresh charge. This assumption is based on using a "perfect displacement" model for scavenging as discussed below. The temperature and pressure rise of the gas during the compression part of the stroke before combustion is determined by the relations for isentropic compression. At the start of combustion, the gas temperature inside the cylinder, T_{i+1}, at time step $i+1$ was calculated using:

$$T_{i+1} = \frac{(q_h - q_v) * m_{fuel\_quantity} * \psi_{combustion\_profile}(\theta_i) - p_i\,[V(\theta_{i+1}) - V(\theta_i)]}{m_{gas}(\theta_i) * c_v} + T_i \tag{2}$$

where q_h = heating value for light diesel fuel, q_v = heat of vaporization for light diesel fuel, $m_{fuel\_quantity}$ = total mass of fuel burned, $\psi_{combustion\_profile}(\theta_i)$ = normalized piece-wise linear combustion profile, $m_{gas}\ (\theta_i) = m_{air} + m_{fuel}\ (\theta_i)$, c_v = constant volume specific heat of air, p_i and T_i = pressure and temperature of air inside the cylinder at the previous time step i, and V = the cylinder volume.

Heat Transfer Coefficient

White [12], similar to Kreith [8], derives the Nusselt number for turbulent flow over a flat plate using the turbulent profile shapes of velocity *u(y)* and temperature *T(y)* in the momentum integral equation for a two-dimensional flat plate boundary layer and in the energy integral relation for a two-dimensional boundary layer:

$$\overline{Nu}_L = \frac{hL}{k} = 0.037\,\mathrm{Re}_L^{0.8}\,\mathrm{Pr}^{1/3} \qquad 0.7 \le \mathrm{Pr} \le 3 \tag{3}$$

where $\overline{Nu}_L$ = mean Nusselt number over characteristic length L, h =heat transfer coefficient, k = thermal conductivity, Re_L = Reynold's number with characteristic length L, Pr =Prandtl number.

Solving for the heat transfer coefficient;

$$h = \frac{.037k}{L}\mathrm{Re}_L^{\,0.8}\,\mathrm{Pr}^{1/3} = \frac{.037k}{L}\left[\frac{\bar{V}L}{\upsilon}\right]^{0.8}\mathrm{Pr}^{1/3} \tag{4}$$

For the temperatures considered here, the Prandtl number was assumed constant at Pr=0.73. The characteristic length L was taken as the cylinder circumference $L = 2\pi * r$. For a forced swirling flow, the velocity was expressed as a tangential velocity at a radius r, $V = \omega * r$. The heat transfer coefficient can then be expressed, as shown in Dent and Sulaiman [7];

$$h = .023\frac{k}{r}\left[\frac{\omega r^2}{\upsilon}\right]^{0.8} \tag{5}$$

Since the gas thermal conductivity and kinematic viscosity are functions of temperature, and the angular velocity of the gas is a function of crank angle (time), h is also function of temperature and crank angle (time);

$$h(T_i, \theta_i) = .023\frac{k(T_i)}{r}\left[\frac{\omega(\theta_i) r^2}{\upsilon(T_i)}\right]^{0.8} \tag{6}$$

The thermal conductivity is a function of temperature, i.e., $k = k(T)$. Many formulations were considered, including a power law formulation, a model that uses a constant Prandtl number equal to a reference value, and Sutherland's Law for molecular viscosity. The function used in this paper is a polynomial curve fit to a data set for 100K to 1600K found in [13]. Any of the other formulations could have been used with minimal effect on the results.

The kinematic viscosity is a function of temperature and crank angle, $\upsilon = \upsilon(T_i, \theta_i)$ such that

$$\upsilon(T_i,\theta_i) = \frac{\mu(T_i)}{\rho(\theta_i)} = \frac{\mu(T_i)}{\left(\frac{m_{gas}(\theta_i)}{Vol_{cyl}(\theta_i)}\right)} \qquad (7)$$

where $m_{gas}(\theta_i) = m_{air} + m_{fuel}(\theta_i)$, $\mu(T_i)$ = dynamic viscosity of air as a function of temperature, and $Vol_{cyl}(\theta_i)$ = trapped cylinder volume as a function of crank angle (time). The function for the dynamic viscosity is based on Sutherland's formula for molecular viscosity.

In the case of a uniflow scavenged opposed-piston engine, the swirl motion of the incoming charge is oftentimes the dominant driver for the heat transfer to the cylinder wall. The swirl motion subsequently decreases throughout the closed cycle due to viscous effects. This effect was modeled in a previous CFD analysis to obtain the angular velocity of the charge as a function of crank angle, namely $\omega(\theta_i) = 2\pi\ N\ SwirlRatio\ (\theta_i)$, where N is the engine speed in revolutions per second (Hertz) and *SwirlRatio* is obtained from a previous CFD analysis.

Using the swirl and fluid property relations discussed above, the heat transfer coefficient for the cylinder wall with bore radius r_b becomes

$$h_w(T_i,\theta_i) = .023\frac{k(T_i)}{r_b}\left[2\pi N r_b^{\,2}\cdot\frac{m_{air}+m_{fuel}(\theta_i)}{Vol_{cyl}(\theta_i)}\cdot\frac{SwirlRatio(\theta_i)}{\mu(T_i)}\right]^{0.8} \qquad (8)$$

Scavenging Model - 'Perfect Displacement'

To model the heat transfer at the intake and exhaust ports, blowdown and scavenging was included. An opposed-piston engine has uniflow scavenging, with burnt gases leaving the exhaust ports and fresh charge entering the intake ports. Sher [14] and Merker et al. [15] give an overview of various scavenging models that have been developed. Scavenging is modeled in this paper using the "perfect displacement" model also known as "plug flow". In this model, a moving planar boundary normal to the cylinder axis moves from the intake port to the exhaust port under the following assumptions:

- No mixing between fresh charge and combustion residuals.
- The incoming fresh charge perfectly displaces the burnt gases.
- There is no mass or heat transfer between the fresh air and burnt gases.
- The pressure is the same on both sides of the partition.

For a given exhaust manifold pressure, the Mach-number of the combustion residuals escaping through the port opening can be approximated using the relations for isentropic flow. Flow through the exhaust port is choked flow at initial port opening and stays at Mach 1 for a period of time. Using the power-law relations for an isentropic gas, the combustion residual density, temperature, and speed of sound of the gas in the exhaust port were calculated. The gas velocity in the port was calculated from the port Mach-number and the speed of sound of the gas in the port.

Having calculated the density, temperature and velocity of the combustion residuals in the exhaust port, the heat transfer coefficient in the port was calculated using

$$h_{exh\_port}(T_i,\theta_i) = .023\frac{k(T_{exh\_port})_i}{r_b}\left[\frac{V_{exh\_port}(\theta_i) * r_b^{\,2} * \rho_{exh\_port}(\theta_i)}{\mu(T_i)}\right]^{0.8} \qquad (9)$$

As blowdown occurs, combustion residuals exit the cylinder. The exposed port area was determined from the total exhaust port opening area, length of the port opening in the cylinder axis direction, and piston crown position as a function of crank angle. The mass of combustion residuals leaving through the port was calculated using the density of the gas in the port, the exposed port area, and velocity of the gas in the port. The mass of combustion residuals left in the cylinder was reduced by the amount of the gas exiting during the current time step. While the intake port is still closed, the volume of the combustion residuals is equal to the cylinder volume. The temperature of the combustion residuals in the cylinder was calculated using the isentropic power-law relations. Knowing the mass, the density and temperature of the combustion residuals still in the cylinder, the heat transfer coefficient for the cylinder wall away from the exhaust port was calculated using equation (8).

Once the intake port opens, and enforcing the condition that the combustion residuals do not mix with the fresh charge, the volume of the fresh charge and combustion residuals are calculated. These volumes change during scavenging depending on the location of the "perfect displacement" partition boundary. Since the scavenging process was treated as isentropic with constant specific heat, the temperature of the combustion residuals remaining in the cylinder could be calculated. Using the ideal gas law, performing a power expansion, and solving for the volume of the combustion residuals, it can be shown that the volume of the combustion residuals is

$$V_E = \frac{m_E \cdot m_{E_0}^{\frac{1}{k}} \cdot T_{E_0}^{\frac{1}{k}} \cdot V_C \cdot V_{E_0} \cdot \rho_{I_0}}{m_E \cdot m_{E_0}^{\frac{1}{k}} \cdot T_{E_0}^{\frac{1}{k}} \cdot \rho_{I_0} + m_{E_0} \cdot m_I \cdot T_{I_0}^{\frac{1}{k}} \cdot V_{E_0}^{\frac{1}{k}} \cdot \rho_{I_0}^{\frac{1}{k}}} \qquad (10)$$

where m_E = mass of combustion residuals, m_{E0} = mass of combustion residuals at exhaust port opening, m_I = mass of

fresh charge, T_{E0} = temperature of combustion residuals at exhaust port opening, $T_{I\ 0}$ = temperature of fresh charge at intake port opening, V_C = total volume of cylinder, V_{E0} = volume of combustion residuals at exhaust port opening, ρ_{I0} = density of fresh charge at intake port opening, and k = specific heat ratio.

With the volume and mass of the combustion residuals in the cylinder known, the density, pressure and temperature of the combustion residuals still in the cylinder can be calculated. With this data, a heat transfer coefficient for the cylinder wall on the exhaust side of the partition can be calculated using equation (8). Likewise, the combustion residual density, temperature and velocity in the exhaust port can be determined and a heat transfer coefficient for the exhaust port can be calculated using equation (9).

Similarly, the temperature of the fresh charge after expansion from manifold conditions into its volume within the cylinder is determined from the isentropic power-law relations. The volume occupied by the fresh charge is the difference between the total volume and that taken up by the combustion residuals. For a given intake manifold pressure and gas density, and since the pressure across the moving partition is constant, the Mach-number of the fresh charge through the intake port can be calculated. The exposed intake port area was determined from the total intake port opening area, the length of the port opening in the cylinder axis direction, and the piston motion. From this, the mass flow into the intake side of the partitioned cylinder can be determined. Together with the fresh charge density and temperature in the cylinder, the heat transfer coefficient for the intake side of the moving partition is calculated from equation (8).

With the intake port Mach-number known, the velocity, temperature and density of the fresh charge in the intake port can be calculated using the isentropic power-law relations. The heat transfer coefficient in the intake ports is determined using

$$h_{\text{int\_ port}}(T_i,\theta_i) = .023\frac{k(T_{\text{int\_ port}})_i}{r_b}\left[\frac{V_{\text{int\_ port}}(\theta_i) * r_b{}^2 * \rho_{\text{int\_ port}}(\theta_i)}{\mu(T_i)}\right]^{0.8} \tag{11}$$

CONVECTIVE HEAT TRANSFER INTO CYLINDER WALL

The cycle averaged heat into the cylinder wall is defined as

$$\overline{Q_w} = \int_{Cycle}\left(\dot{Q}_w\right)dt = \int_{Cycle}\left(\iint_{A_{cyl}}\dot{q}_w dA\right)dt \approx \sum_{Cycle}\sum_{A_{cyl}} h_w(T,\theta)\cdot(T_g - T_w)\cdot\Delta A\cdot\Delta t \tag{12}$$

with A_{cyl} being the exposed surface of the cylinder wall. For a given engine speed N (in Hertz), the time increment can be expressed in terms of a crank angle increment $\Delta\theta_i$ (in degrees),

$$\Delta t = \Delta t(\theta) = \frac{\Delta\theta_i}{360N} \tag{13}$$

Dividing up the cylinder into j annular slices that are Δx_j wide, the surface area becomes

$$A = \sum_{A_{cyl}}\Delta A = \sum_j 2\pi\cdot r_b\cdot\Delta x_j \tag{14}$$

The amount of heat entering into the cylinder wall is then

$$\overline{Q_w} = \sum_i\sum_j h_w(T_{g\,i},\theta_i)(2\pi\cdot r_b\cdot\Delta x_j)(T_{g\,i} - T_{w\,j})\left(\frac{\Delta\theta_i}{360N}\right) \tag{15}$$

The cycle-averaged heat flux as a function of axial position follows directly from the definition of total heat flux in equation (15)

$$\bar{\dot{q}}_w(x_j) = \sum_i h_w(T_{g\,i},\theta_i)(T_{g\,i} - T_{w\,j})\left(\frac{\Delta\theta_i}{360}\right) \tag{16}$$

The summation in equation (16) is only performed whenever the cylinder wall at location x_j is exposed to hot gases. It should be noted that the heat flux in equation (16) is axisymmetric and any effects of potential blow-by past the compression rings are ignored.

Heat Transfer Coefficient as a Function of Cylinder Location and Cycle

The heat transfer coefficient formulation used in equation (16) depends on the location on the cylinder and what part of the cycle the heat into the cylinder is being calculated. During compression, combustion and expansion, equation (8) was used. During blowdown, equation (9) was used for the exhaust port walls and the cylinder bore in the immediate vicinity of the ports. The rest of the discretized cylinder wall used equation (8) with the mass, density and temperature of the combustion residuals calculated as described previously. When the intake port opens and scavenging begins, the partition between the combustion residuals and fresh charge starts to move across the length of the cylinder. Equation (11) was used for the part of the cylinder wall that encompasses the intake port walls. Both the intake and the exhaust side of the moving partition used equation (8) with the mass, density and temperature of either the fresh charge or the combustion residuals, respectively.

Typical Heat Flux Results

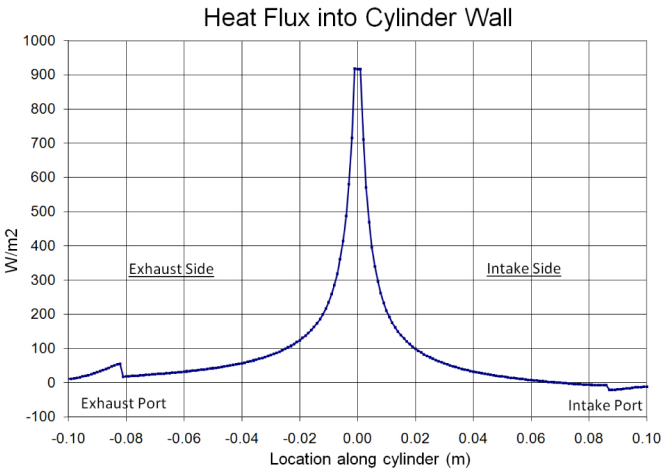

Figure 3. Typical Heat Flux Results

A typical heat flux result is shown in Figure 3 with the exhaust port on the left side and the intake port on the right side. The center of the cylinder (injector plane) is at 0.00 m. The concentration of heat flux in the center region of the cylinder is typical for an opposed-piston engine. The rise in heat flux in the exhaust port area (at location −0.10 to −0.08) is due to the hot gases flowing at high speed through the exhaust port during blowdown. The slightly lower heat flux on the intake side of the cylinder is due to the lower temperature of the incoming fresh charge as scavenging takes place. In the example shown in Figure 3, the low temperature of the incoming fresh charge is actually removing heat from the cylinder in the area of the intake port.

CFD/CHT METHODOLOGY

A solid model of the coolant fluid domain and the cylinder solid domain was created for each design considered. These models were then used in a steady-state Conjugate Heat Transfer (CHT) analysis using heat flux values as boundary conditions on the inner cylinder wall. The fluid inlet boundary conditions were prescribed as flow velocity and were set to 1.5 m/sec. Both the solid and fluid domain initial temperatures were set at 80° C. The fluid domain typically consisted of about 200,000 elements. Meshing for the boundary layer was approximately 250 microns thick constructed of a layer of 10 elements that varied linearly in width from about 10 microns at the innermost element to 50 microns at the outer edge of the boundary layer. The turbulent model used was Shear-Stress-Transport. The solid domain typically consisted on the order of 1.2 million elements. The fluid and solid domain grids were connected using the General Grid Interface (GGI) method in Ansys CFX. The energy imbalance of the fluid domain and solid domain was monitored during the simulations and each simulation was continued until the imbalances fell below 0.3%. Grid dependency studies were not performed, but the grid sizing near the wall followed generally accepted guidelines for the wall coordinate y^+. Temperature dependent material properties were used for the cylinder and coolant. The results of the analysis provided the temperature field throughout the cylinder.

Initial Heat Flux Estimation

The cylinder was discretized into 1 mm wide annular rings and the "time step" was chosen as 0.1 deg crank angle. The heat flux model on the hot side required an estimated wall temperature to calculate an initial heat flux. Either a constant wall temperature or results from a previous analysis were used. The latter aided the rate of convergence of the temperature field.

Iteration of Heat Flux Model and CFD/CHT Analyses

The initial heat flux prediction on the hot side was applied to the inner cylinder wall and port edges as a boundary condition. The temperature results of the cylinder wall from the initial CFD/CHT analysis were then used to update the heat flux prediction. This iterative process of updating the heat flux model and re-running the CFD/CHT analysis was repeated until convergence was achieved. Convergence was defined as less than a 5° C change in the wall temperature between iterations. This typically required two to four iterations. Subsequently, a steady-state thermal analysis was performed on the cylinder solid to evaluate potential bore distortions.

"COOLANT JACKET" STUDIES

A "coolant jacket" approach was studied. The purpose of the design study was to use the heat flux model and CFD/CHT analysis to identify a cooling scheme that would approximate a uniform temperature distribution along the length of the cylinder and circumferentially about the cylinder axis. In addition, a maximum wall temperature target was set at 270° C, in order to ensure engine durability by preserving the oil film in the top ring reversal zone. Engine operating conditions used in the study to estimate heat flux were 170 bar peak cylinder pressure and 3600 rpm engine speed. Due to symmetry, only one quarter of the cylinder and its coolant jacket were analyzed for each design considered. Figures 4,5,6,7,8,9,10,11,12,13,14,15 show the evolution of the design.

Full "Coolant Jacket" Design

The design shown in Figure 4 has the coolant enter a void of uniform thickness on the exhaust side near the exhaust port. The coolant is allowed to flow freely across and around the cylinder OD, although the flow is partially blocked downstream by the injector boss. The flow continues toward the intake port and exits through outlet holes near the ports.

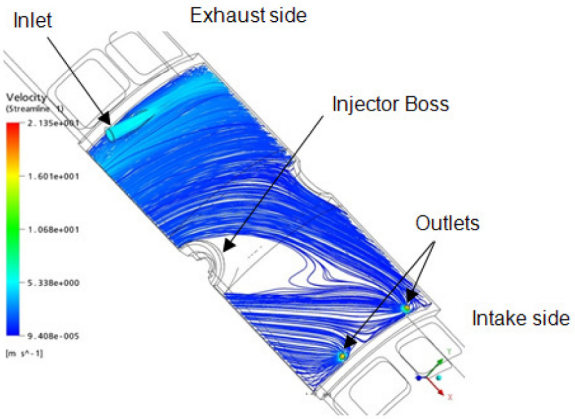

Figure 4. Full "Coolant Jacket" Design

Figure 5 shows the converged CFD/CHT temperature results going down the length of the hot side boundary. These results are from a line on the inner cylinder wall created by the intersection of the inner wall and a plane going through the cylinder axis that is at a 45° angle from the injector boss. As seen in Figure 5, this design created a very uneven temperature distribution, which is not desirable. This is due to the coolant entering from one side of the cylinder (the exhaust side) coupled with a heat flux concentration at the cylinder center. The results show a large axial temperature variation of up to 135° C.

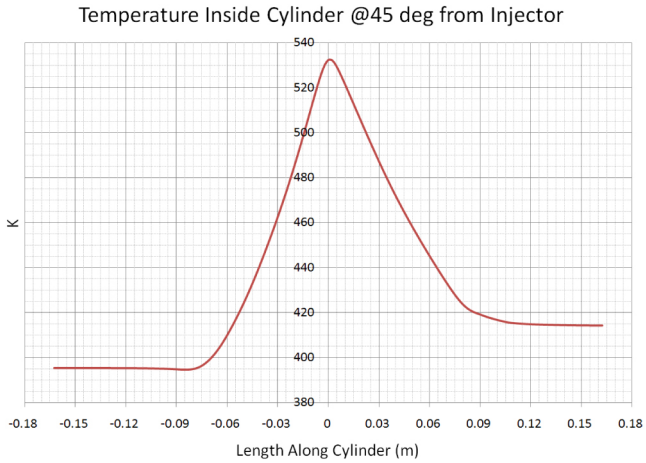

Figure 5. Full "Coolant Jacket" Axial Temperature Results

Figure 6 shows the circumferential temperature results for the inner cylinder wall located on a plane that cuts through the center of the cylinder perpendicular to the cylinder axis. The blocked flow near the injector caused a high circumferential temperature gradient (20° C differential). The poor axial and circumferential temperature distribution warranted no further consideration of this design. The design is presented here to underscore the effects of the concentrated heat load at the cylinder center inherent to opposed-piston engines.

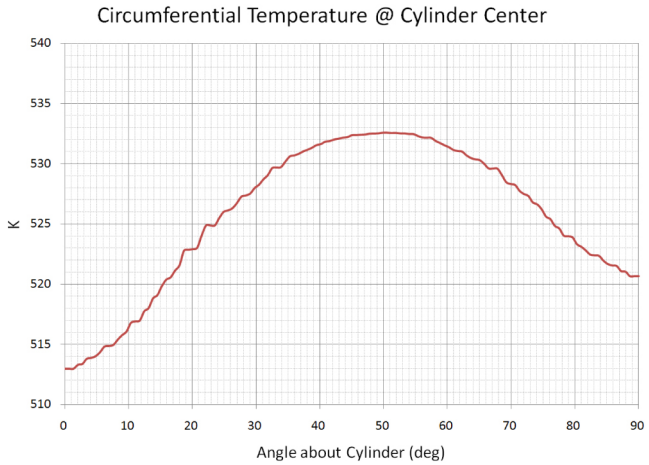

Figure 6. Full "Coolant Jacket" Circumferential Temperature Results

Center "Impingement Jet"/Full Jacket Design

To better address the heat flux concentration at the center of the cylinder, the design in Figure 7 has an inlet at the cylinder center that acts as an "impingement jet". The coolant impinges directly on the cylinder wall creating a stagnation flow field. The flow continues longitudinally down the exhaust side and intake side of the cylinder and exits through outlet holes near the ports.

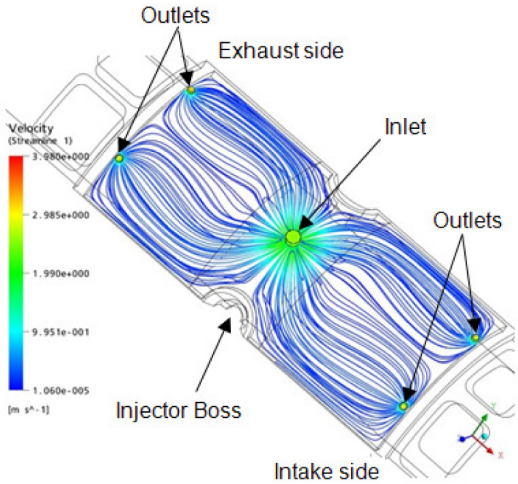

Figure 7. Center "Impingement Jet"/Full Jacket Design

Similar to the first design, both ends of the cylinder are "overcooled" as shown in Figure 8. The axial temperature variation is 60° C on the exhaust side and about 90° C on the intake side causing a highly uneven thermal expansion along the length of the cylinder. Figure 9 shows a localized "cold" spot due to the impingement jet. However, the circumferential temperature variation was only 9° C in this design as compared to 20° C in the previous design. These results show that impingement cooling at the center of the

cylinder could improve the cooling around the injector boss and, therefore, promote circumferential temperature uniformity.

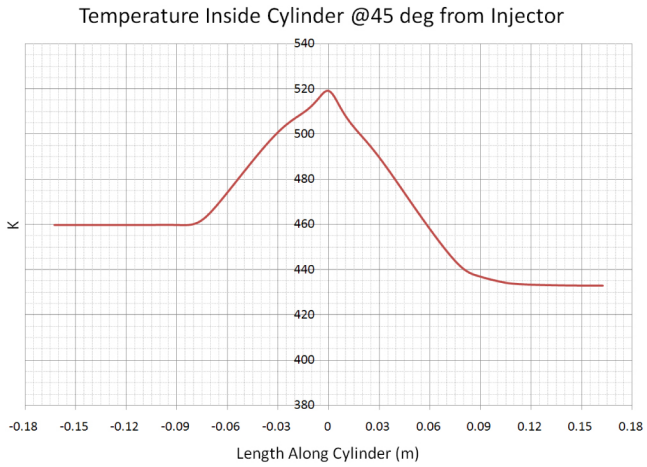

Figure 8. Center "Impingement Jet"/Full Jacket Design Axial Temperature Results

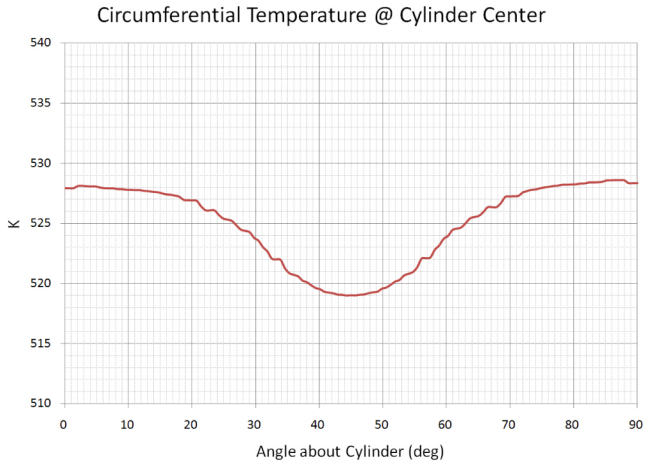

Figure 9. Center "Impingement Jet"/Full Jacket Design Circumferential Temperature Results

Center "Impingement Jet"/Shortened Jacket Design

To address the previously mentioned overcooling effect at both ends of the cylinder, the coolant jacket was shortened. The jacket length on the exhaust side was kept slightly longer than on the intake side to account for uneven heat flux between the exhaust and intake side. With the outlets located near the injector bosses, some of the flow is forced to circulate around the bosses.

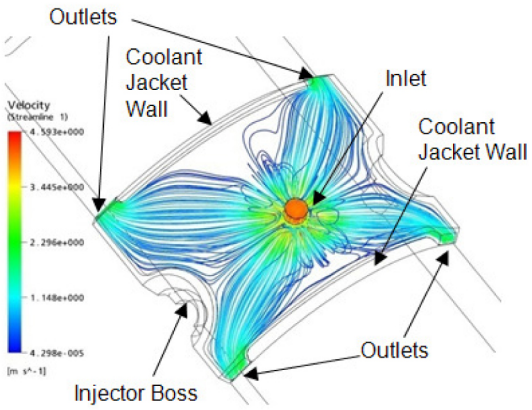

Figure 10. Center "Impingement Jet"/Shortened Jacket Design

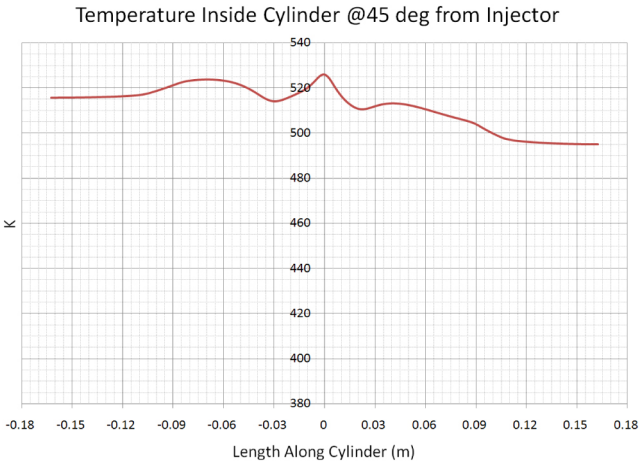

Figure 11. Center "Impingement Jet"/Shortened Jacket Design Axial Temperature Results

This design showed significant improvement in reducing overcooling the ends of the cylinder. The axial temperature variation is reduced to 30° C compared to the 60-90° C differential from the previous design and 135° C from the original full "coolant jacket" design. The two dips in temperature at the −.03 m and +.025 m locations were caused by extra cooling from stagnation flow occurring at either end of the coolant jacket at a location halfway between the outlets. The temperature of the intake side could be raised by further shortening the length the coolant jacket on this side of the cylinder. The circumferential temperature variation shown in Figure 12 is about 10° C and is similar to the previous design, indicating that the thermal response of the cylinder in axial direction is largely decoupled from the response in circumferential direction.

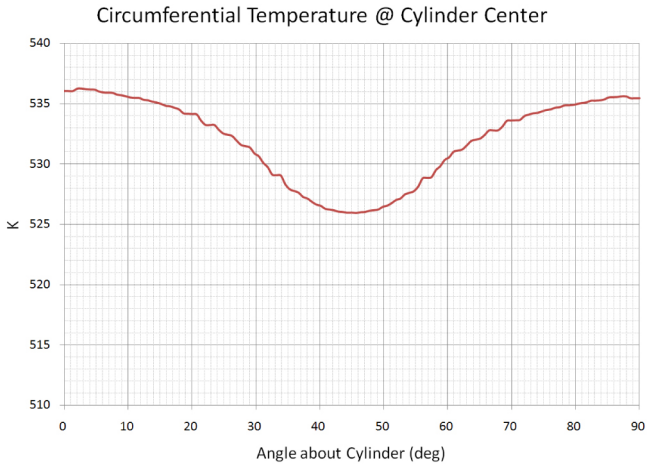

Figure 12. Center "Impingement Jet"/Shortened Jacket Design Circumferential Temperature Results

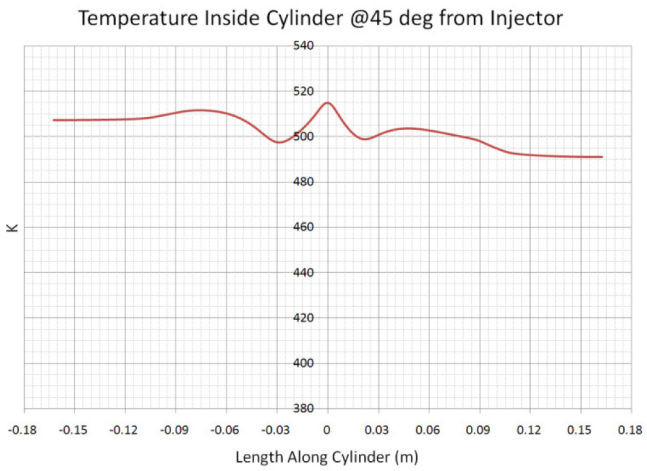

Figure 14. Slotted Center Impingement Design Axial Temperature Results

Slotted Center Impingement Design

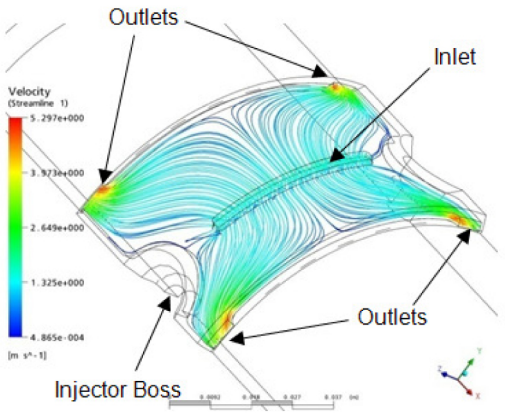

Figure 13. Slotted Center Impingement Design

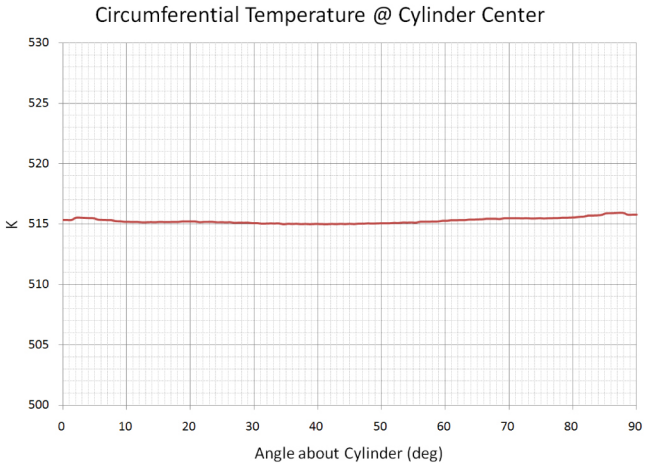

Figure 15. Slotted Center Impingement Design Circumferential Temperature Results

To further improve the circumferential temperature distribution, the single circular inlet was changed to a slot. The coolant jacket length remained the same as in the previous design.

This design shows significant improvement in the circumferential temperature distribution (Figure 15). The temperature variation is 1° C compared to the 9-10° C variation of the previous two designs and 20° C variation of the first design. The axial temperature distribution and variation shown in Figure 14 are similar to the previous design shown in Figure 11, further indicating that circumferential temperature control is largely independent of axial temperature control.

Subsequently, a steady-state thermal analysis was performed on this design to determine the thermal expansion. The results showed the axial expansion to be reasonably uniform with a maximum variation of 40 microns over the entire length of the cylinder. The circumferential variation at the center of the cylinder, and 3mm to either side of the center plane, was 5 microns.

Design Study Findings

The findings from the design study were significant:

• A coolant jacket design that uses a large surface area is susceptible to uneven cooling and possibly overheating of the coolant in the boundary layer.

• A coolant jacket that extends only part way down the length of the cylinder is beneficial in preventing over-cooling of the cylinder ends and provides control over the axial temperature distribution.

• Circumferential temperature control is best accomplished by distributed impingement flow at the cylinder center (injector plane).

• Axial temperature control is largely independent of circumferential temperature control.

IMPLEMENTATION OF DESIGN STUDY FINDINGS

The first step in implementing the design study findings was to convert the inlet slot into discreet impingement jets by inlaying a thin steel band with small holes, called an impingement band, into the cylinder. To ensure the flow through all of the jets was balanced, the size of the hole diameters were varied as necessary. The coolant jacket that extended down the exhaust side was converted to a series of independent grooved channels in the cylinder that were lined up with every other impingement jet. The coolant jacket on the intake side was also converted to independent grooved channels, which were lined up with the impingement jets not associated with the exhaust side. The purpose in aligning a grooved channel to an impingement jet was for better flow control. The length of the channels on the exhaust side were longer than those on the intake side to account for the difference in heat flux from side to side as predicted by the heat flux model. The length of the channels on each side was determined by repeated CFD/CHT analysis as described above. The intention was to create a small impingement jet on the cylinder center at each hole in the impingement band, guide that flow down the length of the cylinder for some distance, and then empty the coolant out into a collector groove in the block. To feed the impingement jets, an annulus, called the supply groove, was machined into the block that, in turn, was fed by the main coolant supply. At the end of each channel in the cylinder, the coolant exited into an annulus cut in the block on the exhaust side and the intake side (called the exhaust side outlet groove and intake side outlet groove, respectively) that acted as collectors. Analysis showed the exhaust bridges needed to be cooled. To do this, select channels in the cylinder on the exhaust side were extended to the exhaust ports until they intersected with a cross-drilling. This cross-drilling also intersects with a hole that goes through the exhaust bridge. Figures 16,17,18 show the resulting design, which is referenced in [16];

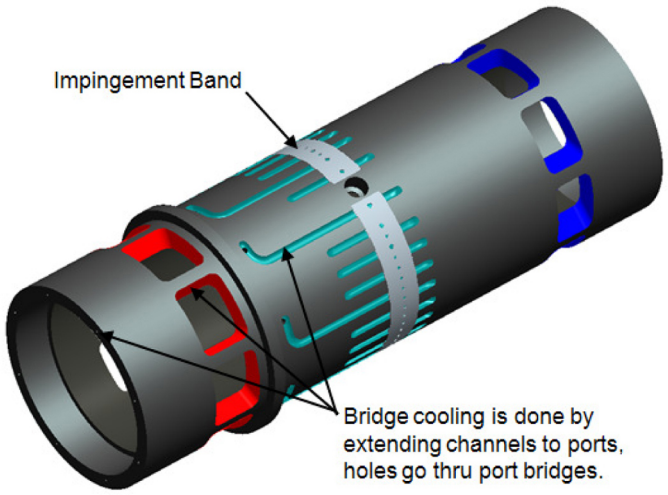

Figure 16. Cylinder with Impingement Band

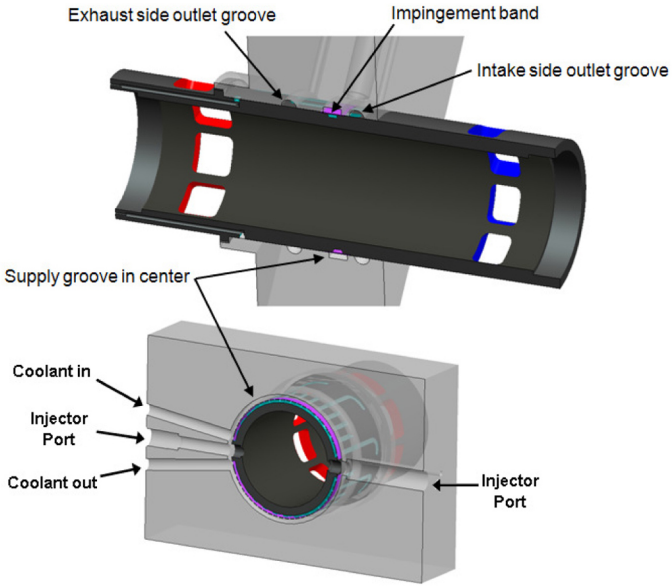

Figure 17. Block Grooves

The converged heat flux into the cylinder wall and ports for this design are shown in Figures 18 and 19.

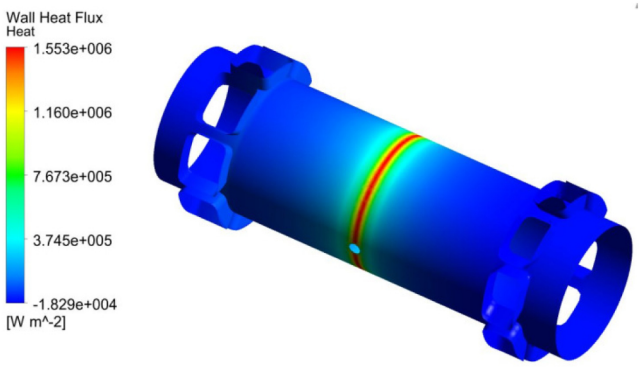

Figure 18. Heat Flux Boundary Condition for CFD/CHT Analysis

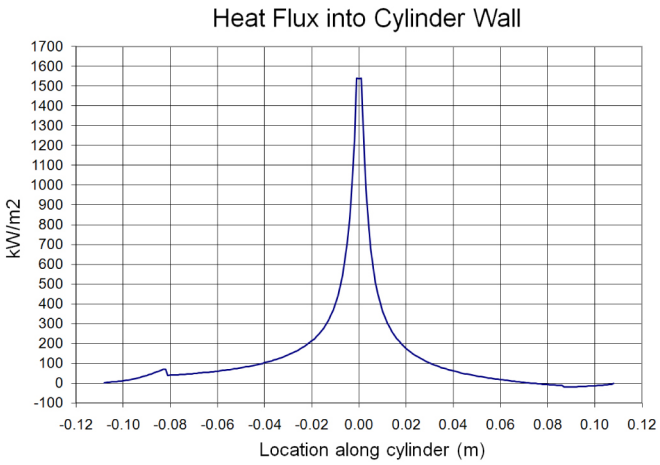

Figure 19. Plot of Heat Flux Boundary Conditions

The results from the CFD/CHT analysis are shown below.

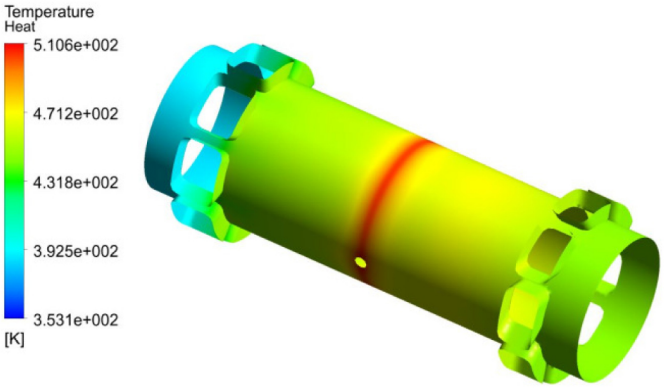

Figure 20. CFD/CHT Temperature Results

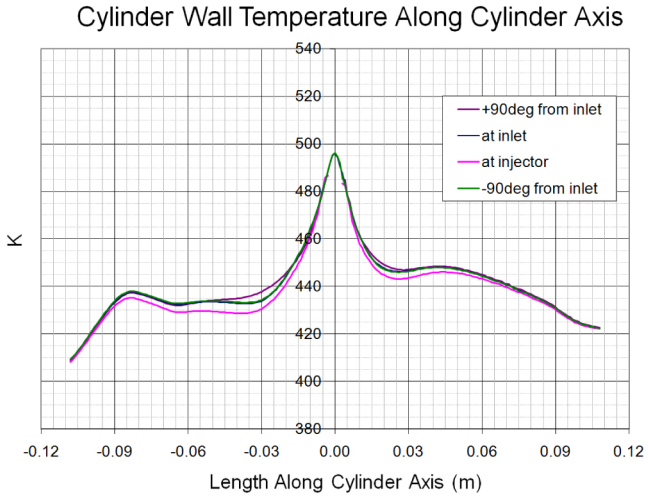

Figure 21. Axial Temperature Results

The temperature results shown in Figures 20 and 21 indicate a maximum temperature of 215° C concentrated at the center of the cylinder. The temperature toward the exhaust port and intake port are relatively constant. The overall temperature differential is on the order of 60° C.

To level the overall temperature response and reduce the axial temperature differential, shorter channel lengths in the cylinder for both the exhaust side and the intake side would be needed. However, the physical constraint of putting the supply grooves and collector grooves in the block closer together come into play. Note that the bridge cooling reduced the cylinder wall temperature at the exhaust end of the cylinder. The magnitude of circumferential temperature variations at various axial locations can be seen in Figure 21.

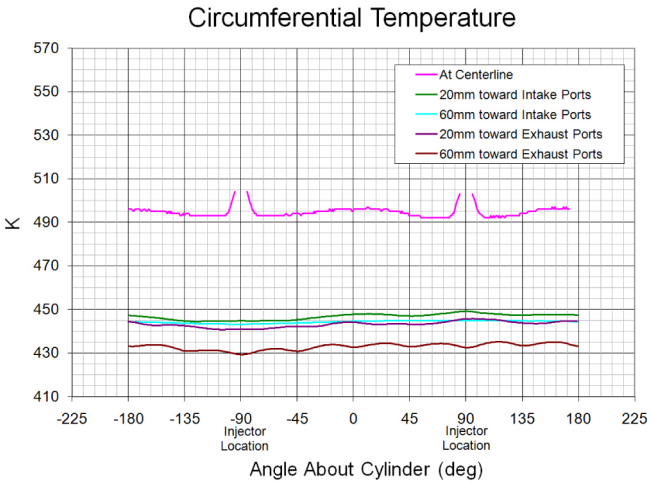

Figure 22. Circumferential Temperature Results

Figure 22 shows the circumferential temperature results to be within 5° C at the cylinder centerline except for the injector boss locations. The temperature rises quite dramatically at the

injector boss locations, suggesting more focused cooling around the bosses is needed. Figure 22 also shows the circumferential temperature at locations 20 mm and 60 mm away from the cylinder center, both toward the exhaust ports and intake ports. These are all within a 5° C variation also.

EXPERIMENTAL VALIDATION

The cylinder configuration introduced in the previous section was subsequently fabricated and run in a single-cylinder, opposed-piston prototype engine. In order to validate the cylinder cooling performance of the new cooling approach, several thermocouples were embedded into the cylinder. One set of thermocouples was placed in between the cylinder center (injector plane) designated by coordinate '0' in Figure 23 and the exhaust ports in the direction of the cylinder axis. The exhaust side of the cylinder was chosen because this part of the cylinder typically runs hotter compared to the intake side and warrants special attention. The results of the comparison between simulations and measurements are shown in Figure 23. It should be noted that the thermocouples were embedded in the cylinder wall about 2 mm from the inner surface of the cylinder. This placement of the thermocouples significantly reduced the total measured temperature variation compared to the variation of the temperature on the surface of the combustion chamber referenced in the previous sections.

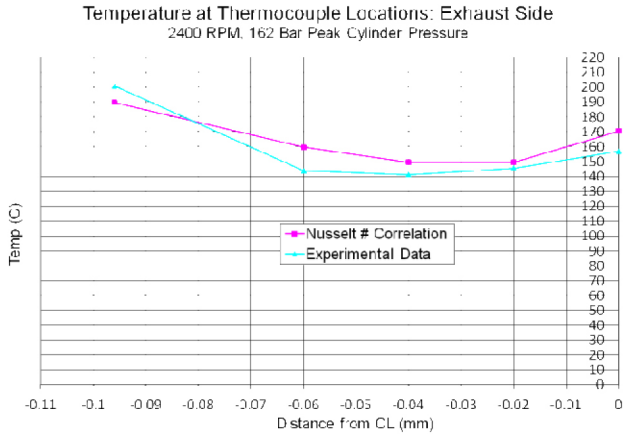

Figure 23. Comparison with Experimental Data: Exhaust Side

A second set of thermocouples was placed around the circumference of the cylinder at the cylinder center line (injector plane), which is the region of the highest heat input (see Figure19). The results are shown in Figure 24 and indicate good agreement between simulation and temperature measurements.

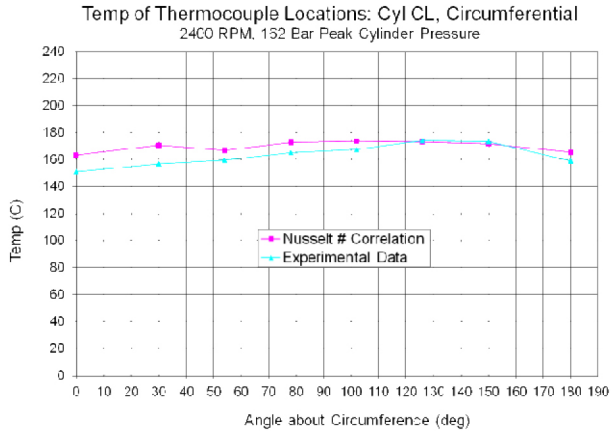

Figure 24. Comparison with Experimental Data: Cylinder Center Line (Injector Plane)

SUMMARY

A heat flux model has been created to predict the heal flux distribution into the cylinder wall and ports based on a discretized Nusselt number correlation for the heat transfer coefficients The gas temperature during compression and combustion is determined by a single zone thermodynamic model. Blowdown and scavenging is modeled using a perfect displacement model. The cylinder has been discretized into 1 mm wide annular slices and a cycle-averaged heat flux value for each slice has been calculated. The cycle averaged heat flux values are used as hot side boundary conditions in a Conjugate Heat Transfer (CHT) analysis of the cylinder solid domain and the coolant fluid domain. Results from the CHT analysis provide the temperature field in the cylinder and the cylinder wall.

Cylinder wall temperatures are fed back into the heat flux model to update the heat flux prediction. Convergence between the heat flux model and CHT results for the cylinder wall usually require two to four iterations.

Based on this analysis method, a cylinder cooling design study was conducted for various types of "coolant jacket" designs. The study led to the discovery of a unique approach to cylinder cooling for opposed-piston engines. The cylinder thermal response has been greatly improved by introducing coolant, in the form of "impingement jets", to the hot center section of the cylinder. After impingement, the coolant is directed by a discrete number of axial channels along the outer cylinder wall toward either end of the cylinder. Circumferential temperatures are shown to be within 5° C around the cylinder. Axial temperatures are well below the target temperature of 270° C. Over-cooling of the cylinder ends is controlled by limiting how far the flow extends longitudinally along each side of the cylinder. The heating of exhaust post bridges from hot gases exiting the exhaust port are controlled by coolant passages through the bridges.

Furthermore, a comparison between measured and simulated data shows good agreement suggesting that the proposed method represents an expedient and sufficiently accurate technique for performing cylinder cooling design studies.

CONCLUSION

The discretized Nusselt number correlation approach represents an expedient method for estimating heat flux for input into a CHT analysis. This methodology provided directional guidance during the evaluation of several design concepts and led to the development of a new and efficient cylinder cooling approach for opposed-piston engines. Distributed impingement flow at the cylinder center plane allowed for circumferential temperature control. Limiting the length of coolant flow along the length of the cylinder provided control over the axial temperature distribution. The simulation and experimental results indicate that engine durability can be enhanced by providing thermal control over the cylinder and creating acceptable liner temperatures for oil film preservation and minimizing bore distortions.

ACKNOWLEDGEMENT

The authors would like to thank William McHargue for his helpful advice on modeling the mass transport during blowdown and scavenging.

REFERENCES

1. Flint, M.L.S. and Pirault, J.-P., "Opposed Piston Engines: Evolution, Use, and Future Applications," SAE International, Warrendale, PA, ISBN 978-0-7680-1800-4, 2009, doi: 10.4271/R-378.

2. Barsanti, E. and Matteucci, F., "Motore a Pistoni Contrapposti", Piedmont Patent 700, July 26, 1858.

3. Barsanti, E. and Matteucci, F., "Improved Apparatus for Obtaining Motive Power from Explosive Compounds", Great Britain Patent 3270, December 31, 1861.

4. Regner, G., Herold, R., Wahl, M., Dion, E. et al., "The Achates Power Opposed-Piston Two-Stroke Engine: Performance and Emissions Results in a Medium-Duty Application," *SAE Int. J. Engines* 4(3):2726-2735, 2011, doi: 10.4271/2011-01-2221.

5. Junkers, H., "Cylinder of Internal-Combustion Engines and Other Similar Machines", U.S. Patent 1 231 903, July 3, 1917.

6. Junkers, H., "Engine", U.S. Patent 2 031 318, February 18, 1936.

7. Dent, J. and Sulaiman, S., "Convective and Radiative Heat Transfer in a High Swirl Direct Injection Diesel Engine," SAE Technical Paper 770407, 1977, doi: 10.4271/770407.

8. Kreith, F., "Principles of Heat Transfer", 2nd Edition, International Textbook Co., Scranton, 1969, page 314.

9. Annand, W.J.D., "Heat Transfer in the Cylinders of Reciprocating Internal Combustion Engines" Proc. Inst. Mech. Engrs., Vol. 177, No. 36, 1963, pg. 973.

10. Woschni, G., "A Universally Applicable Equation for the Instantaneous Heat Transfer Coefficient in the Internal Combustion Engine," SAE Technical Paper 670931, 1967, doi: 10.4271/670931.

11. LeFeuvre, T., Myers, P., and Uyehara, O., "Experimental Instantaneous Heat Fluxes in a Diesel Engine and Their Correlation," SAE Technical Paper 690464, 1969, doi: 10.4271/690464.

12. White, F., "Heat and Mass Transfer", Addison-Wesley Publishing Company, Inc., 1991, page 324.

13. Society of Fire Protection Engineers. "SFPE Handbook of Fire Protection Engineering", National Fire Protection Association, 2nd Edition, 1995. Table B-2.

14. Sher, E., "Modeling the Scavenging Process in the Two-Stroke Engine-An Overview," SAE Technical Paper 890414, 1989, doi: 10.4271/890414.

15. Merker, G. and Gerstle, M., "Evaluation on Two Stroke Engines Scavenging Models," SAE Technical Paper 970358, 1997, doi: 10.4271/970358.

16. Lemke et al., "Cylinder And Piston Assemblies For Opposed Piston Engines", Patent Application Publication US2010/0212637.

CONTACT INFORMATION

Patrick R. Lee
lee@achatespower.com

Michael H. Wahl
wahl@achatespower.com

ISSN 0148-7191

SAE Customer Service:
Tel: 877-606-7323 (inside USA and Canada)
Tel: 724-776-4970 (outside USA)
Fax: 724-776-0790
Email: CustomerService@sae.org
SAE Web Address: http://www.sae.org
Printed in USA